HTML ABSTRACT + LINKS

JOURNAL OF APPLIED PHYSICS 97, 023525 (2005)

Evolution of in-plane texture in reactively sputtered CrN films

Z. B. Zhao[a)]
Delphi Research Labs, 51786 Shelby Parkway, Shelby Township, Michigan 48315

Z. U. Rek
Stanford Synchrotron Radiation Laboratory, Stanford University, California 94309

S. M. Yalisove and J. C. Bilello
Department of Materials Science and Engineering, The University of Michigan, Ann Arbor, Michigan 48109

(Received 9 July 2004; accepted 29 September 2004; published online 27 December 2004)

The microstructure and texture of chromium nitride films reactively sputtered on silicon substrates were investigated using x-ray scattering, pole figures, transmission electron microscopy, and atomic force microscopy. Under the given deposition geometry, the CrN films were shown to develop a in-plane texture. The three preferred crystallographic orientations of the CrN films approximately coincided with the characteristic directions associated with the deposition geometry. There appear to be two regimes that govern the microstructural evolution and texture development for reactively sputtered chromium films. The first one involves the deposition conditions that lead to the formation of a single, stable phase such as stöichiometric CrN (above certain level of nitrogen partial pressure). In this regime, the film growth appears to be controlled by local epitaxy in individual columns, competitive grain growth, and kinetic roughening. The film characteristics resulted from this regime include the development of the in-plane texture, well-organized microstructures with relatively coarse grains, increased surface roughness, and large tensile stress. The second regime involves the transitional region prior to formation of the stable phase CrN in which significant microstructural refinements take place. This transitional region is associated with the thermodynamically metastable phase CrN_x or the presence of multiple phases. The continuous renucleations during film growth disrupt the local epitaxy and impede kinetic roughening. This leads to film characteristics manifested by weakened or no texture, ultrafine microstructure (e.g., nanocrystalline structures), reduced surface roughness, and a tendency for residual stress to transit from tensile to compressive. © *2005 American Institute of Physics*. [DOI: 10.1063/1.1823022]

I. INTRODUCTION

Polycrystalline thin films grown by vapor depositions frequently develop crystallographic textures.[1,2] Understanding and control of film texture structure is important because the properties of the films (mechanical, electrical, magnetic, and optical) and their functional performance can be strongly dependent on the net crystallographic orientations of the film grains. TiN thin films, for example, possess increased wear resistance as tribological coatings if they are (111) textured[3] Also, the reliability of metallizations in VLSI circuits is directly related to the texture structure of metal interconnects.[4] For thin films used for magnetic recording media, certain textures can be deliberately promoted to enhance their performance.[5,6] Vapor deposited films usually possess only out-of-plane textures, i.e., a primary crystallographic axis orients preferentially along the direction of film growth, while the grains are still randomly oriented in the plane of film.[7,8] Under certain conditions, in-plane textures can also be present in sputter deposited films. For example, the in-plane textures were observed in films deposited using electron beam or evaporation techniques under the influence of ion bombardment at an oblique angle.[9,10] The mechanism for this growth behavior was explained to be the result of preferential sputtering yields for grains of different crystallographic orientations. Strong in-plane textures were also found to occur in magnetron sputtered Mo films,[11] Cr films,[12] and Mo/W multilayers,[13,14] when grown on moving substrates that repetitively passed through a plasma cloud at regular intervals. This was attributed primarily to the self-shadowing effect and anisotropic grain growth, and a mathematical model was developed to explain the nature of in-plane textures.[15] All previous studies on in-plane textures were focused on metal thin films.[9–13] For the films deposited via reactive sputtering, the reactive species in the sputter chamber presents an additional variable that can strongly affect microstructural evolution.[16] It is not clear whether the in-plane texture can be similarly developed in compound thin films grown via reactive sputtering. The present study characterizes reactively sputtered CrN films prepared under a similar deposition geometry in which the metal films develop in-plane textures.[11,12] By examining the effects of the reactive species in reactive sputtering, we were able to generate some insights into the growth mechanisms that govern texture development, microstructural evolution, and other related film characteristics.

II. EXPERIMENTAL PROCEDURES

All CrN films were deposited onto native oxides of (100) Si single crystal wafers via direct current (dc) reactive mag-

[a)]Electronic mail: zhibo.zhao@delphi.com

 © 2005 American Institute of Physics

netron sputtering. The schematic of the deposition geometry was shown previously.[12] In such a configuration, multiple Si wafer substrates were mounted on a platen which rotates at a constant 20 rpm. The center of each substrate was about 25 cm from the axis of the platen. The Si substrates were consistently placed in a manner such that their [110] flat edges were nearly parallel to the radial direction of the rotating platen. For an individual substrate, the film deposition took place only during the moments that the substrate passed through the plasma cloud. Accordingly, the film growth occurred repetitively at regular intervals. All CrN films were deposited by sputtering a pure Cr target, which was placed vertically 6 cm over the substrates. The chamber base pressures were typically less than 1×10^{-6} Torr. Prior to a deposition, the Cr target was always presputtered for 5 min to remove the surface oxides, and reduce the introduction of impurities into the films. All CrN films were deposited at cathode power of 460 W and 2 mTorr Ar partial pressure, with the nitrogen partial pressure varying from 0.2–2.8 mTorr.

X-ray scattering experiments were conducted at the 7-2 Beamline of the Stanford Synchrotron Radiation Laboratory (SSRL) under standard conditions (3 GeV and 100 mA at fill). The monochromatic x-ray with wavelength 0.124 nm (10 keV) was selected through a Si(111) double-crystal monochromator. The horizontal divergence and vertical divergence of the beam were 3 mrad and 0.2 mrad, respectively. The incident beam was defined by a 1 mm$\times$1 mm slit. The [110] flat edges of (100) Si substrates were used to orient the substrates consistently with respect to the incident beam. In order to eliminate the effects of beam instabilities and beam decay as a function of time, all the experiments were conducted in the "dose" mode. In this mode, the intensities of both the incident beam and the diffracted beam were detected by two synchronized detectors, which ensures equal x-ray dose for each collection of the diffraction intensity. Such dose mode is commonly used for long x-ray data collections with decaying (fluctuating) incident beam. Symmetric grazing incidence x-ray scattering (GIXS) was used to collect the reflection intensities from the lattice planes that are nearly parallel to the plane of a film. For an individual scan, both incident and exit beams were kept at approximately 1° with respect to the film surface. Further details of the experimental setups and x-ray beam conditions used for the symmetric GIXS experiments were given in a previous paper.[12]

For a given CrN film specimen, the 2θ scan with symmetric GIXS was performed to establish the Bragg conditions for several major reflections, including (110), (111), (200), and (113). Subsequently, the specimen was rotated along its surface normal, in order to collect the in-plane intensity distributions of certain characteristic reflections as functions of the azimuthal angles ϕ (0°–360° with 2° per step). The diffraction intensity at any ϕ is directly proportional to the volume fraction of the grains which have a particular in-plane orientation defined by the given diffraction vector. Therefore, such ϕ scans with symmetric GIXS geometry directly generate information on in-plane preferential crystallographic orientations for the film specimen.

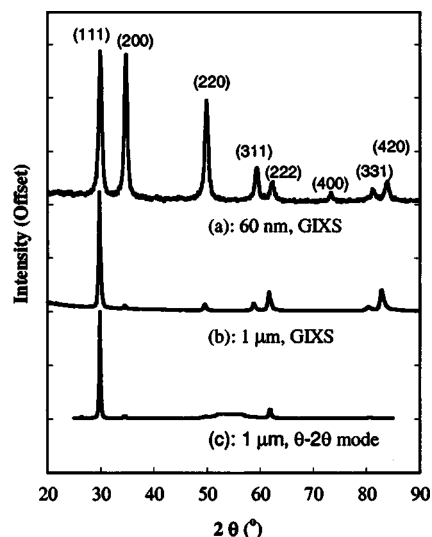

FIG. 1. X-ray diffraction patterns of the CrN films deposited at 460 W, 2 mTorr Ar, and 1.2 mTorr nitrogen. (a) The pattern of a 60 nm thick CrN film, obtained via the symmetric GIXS. (b) The pattern of a 1 μm thick film, obtained via the symmetric GIXS. (c) The pattern of the 1 μm film, obtained via the $\theta-2\theta$ symmetric reflection geometry.

The pole figures of the CrN films were collected using a Rigaku Rotaflex x-ray system equipped with a 12 kW rotating anode x-ray source (Cu Kα radiation) and a Rigaku texture diffractometer configured in the Schultz geometry. In the preparation of thin foils for transmission electron microscopic (TEM) observations, the samples were ultrasonically cut, mechanically back thinned to ~125 μm and chemical etched to perforation using a HNO_3:HF:CH_3COOH mixture (3:5:3). Additional ion milling (Ar^+ ions at 5 keV) was performed to produce electron transparent regions in the specimens. Since the sample preparation involved thinning from the backside, electron transparent regions were produced near the top ~50 nm of a film. The surface morphologies of the CrN films were observed using a Digital Instruments NanoScope III atomic force microscope (AFM). The tapping™ mode was used and the surface plots were digitized in 512$\times$512 pixel arrays. All images were taken from 2000×2000 nm^2 regions with a scanning frequency of ≈1.5 Hz.

III. EXPERIMENTAL RESULTS

A. Triaxial nature of the texture in the CrN films

Figure 1(a) shows the symmetric GIXS diffraction pattern of a 60 nm thick film deposited at 460 W, 2 mTorr Ar partial pressure, and 1.2 mTorr nitrogen partial pressure. The pattern, which can be readily indexed as a cubic lattice, indicates that the formation of a single phase of CrN. Since the diffraction pattern in Fig. 1(a) exhibits similar reflection intensity ratios to those reported by the International Center for Diffraction Data (ICDD) for the bulk polycrystalline Cr samples, one assumes that the grains in this "thin" film are largely randomly oriented. Figure 1(b) shows the symmetric GIXS diffraction pattern of a 1 μm film deposited at the same conditions as the 60 nm film. Note that the diffraction vectors for the reflections in the GIXS pattern are nearly

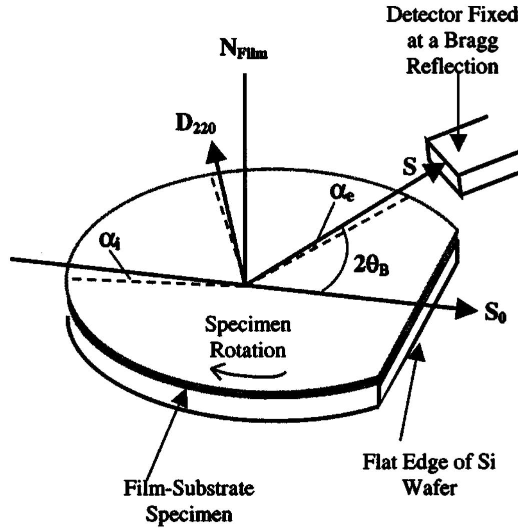

FIG. 2. A schematic showing the setup for an azimuthal (ϕ) scan. In the drawing, the ϕ scan of the (220) reflection is illustrated as an example. Note that the three dashed lines are the lines in the plane of the film. The incident beam ($\mathbf{S_0}$), the exit beam ($\mathbf{S}$), and the diffraction vector $\mathbf{D_{220}}$ form grazing angles with the dashed lines, respectively. The detector is fixed at a predetermined Bragg reflection condition and the diffraction intensity is then collected while the sample is rotated along its normal ($\mathbf{N_{Film}}$) from 0° to 360°. The [110] flat edge of Si wafer is used as the reference for the starting position of a ϕ scan.

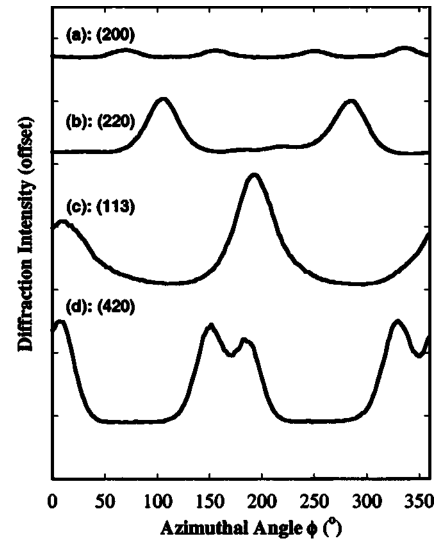

FIG. 3. Selected examples of ϕ scan results for the 1 μm thick CrN film deposited at 460 W, 2 mTorr Ar partial pressure, and 1.2 mTorr nitrogen partial pressure.

parallel to the film plane. The distinct features between Figs. 1(a) and 1(b) are indicative of the presence of in-plane preferred orientations for the thicker film. In addition, the diffraction pattern of the thicker film in Fig. 3(c), obtained via θ–2θ symmetric reflection geometry, shows the presence of preferred [111] orientation in the direction of film growth, namely, the (111) type out-of-plane texture.

From the diffraction pattern in Fig. 1(b), the Bragg conditions for various reflections of the CrN film were first established as $2\theta=30.02°$ for (111), $2\theta=34.90°$ for (200), $2\theta=50.15°$ for (220), $2\theta=59.53°$ for (113), and $2\theta=84.07°$ for (420). The diffraction intensities were also collected as a function of the azimuthal angle (i.e., ϕ scans). The experimental setup for the ϕ scan of the (220) reflection is shown schematically in Fig. 2. The [110] flat edge of Si substrate was used as the reference for marking the starting position of specimen rotation. The results of ϕ scans for the 1 μm film, of Fig. 1(b), are shown in Fig. 3. The variations of the diffraction intensities are clearly indicative of the presence of preferred crystallographic orientations in the plane of the film. It should be pointed out that the diffraction intensities were not contributed from the entire thickness of the 1 μm film due to the grazing incidence angles of the incident and diffracted beams. The kinematical depth of penetration can be readily derived as

$$t_p=\frac{\sin(\alpha_i)\sin(\alpha_e)}{\mu(\lambda)[\sin(\alpha_i)+\sin(\alpha_e)]},$$

where $\mu(\lambda)$ is the linear absorption coefficient, λ is wavelength, and α_i and α_e are, respectively, the angles formed by the incident and exit beams to the surface of the thin film specimen. Based on the grazing angles used in this work, it can be estimated that diffraction intensities shown in Fig. 3 are primarily from the top layer of ~150 nm of the CrN film.

Let us examine the intensity distributions of the commonly observed reflections of CrN as functions of the azimuthal angle ϕ. It is noted that the diffraction intensities of the (200), (311), and (420) reflections are either low in magnitude fluctuations or asymmetric. This is mainly due to the fact that the film is (111) textured in the direction of film growth. In other words, the grains in such a film oriented predominantly in such a way that their {111} planes were nearly parallel to the plane of the film. Thus, there are few grains whose {200}, {311}, {420}, and {111} planes that are perpendicular to the plane of the film since these crystallographic planes are not orthogonal to {111} planes in a cubic lattice. However, the (220) plane is orthogonal to {111} plane. Accordingly, the intensity distribution of the (220) reflection is best suited for revealing the in-plane texture structure. Based on the analysis of the diffraction patterns in Fig. 1 and the results of the ϕ scan in Fig. 3, it can be deduced that the ⟨110⟩ crystallographic orientation aligns preferentially along the tangential direction (or the direction of rotation). Furthermore, one can derive that the preferred orientation along the radial direction is ⟨112⟩. Now, the structure of the texture and its correlation with the deposition geometry can be depicted in Fig. 4. Clearly, the texture in the CrN film is triaxial in nature, namely, the three preferred crystallographic orientations coincide with the characteristic directions associated with the deposition geometry. It should be pointed out that the preferred orientations of the textured CrN films are actually not aligned *precisely* with the three-characteristic directions related to the deposition geometry. In fact, the preferred [111] orientation deviates by 5°–10° from the sample normal (i.e., the direction of growth), as revealed by the pole figures shown in Sec. III C.

B. Evolution of texture: thickness dependence

The evolving behavior of the texture was further studied by examining the CrN films with three nominal thicknesses,

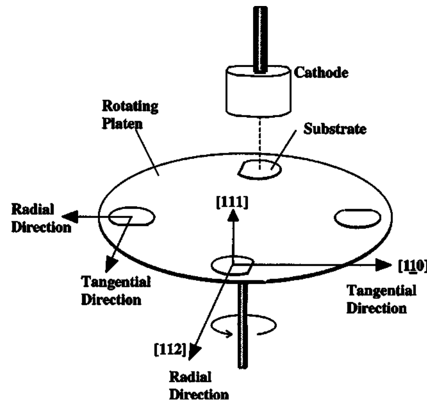

FIG. 4. A schematic depicting the structure of the triaxial texture in the CrN film in relation to the deposition geometry. The triaxial texture is denoted by three preferred orientations [111], [110], and [112], while the characteristic directions of the deposition are represented by the radial direction and the tangential direction (i.e., the direction of rotation).

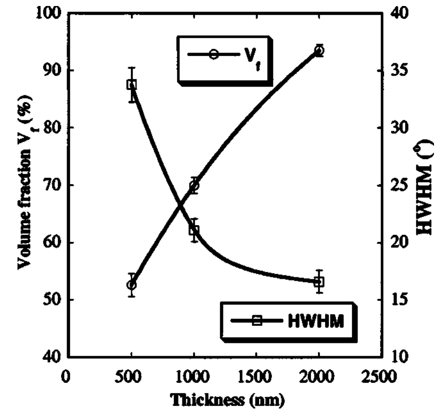

FIG. 6. Evolution of the in-plane texture in the CrN film deposited at nitrogen partial pressure of 1.2 mTorr as a function of thickness, as indicated by the volume fraction V_f and the HWHM. Due to the grazing angle used in the ϕ scans, the data represent the results from the ~150 nm top layers of the films.

0.5-μm, 1-μm, and 2-μm. All these films were deposited at the same conditions, 460 W, 2 mTorr Ar partial pressure and 1.2 mTorr nitrogen partial pressure. The diffraction results from the symmetric θ–2θ symmetric reflection geometry indicate that the 0.5 μm and 2 μm films have the [111] preferred orientation in the direction of film growth, similar to the 1 μm film described in Sec. III A. The ϕ scan results of the (220) reflection, shown in Fig. 5, suggest that the CrN films with varying thickness developed the same type texture as denoted in Fig. 4. Of all the available Bragg reflections for the CrN films, only the (220) reflection is best suited to characterize the in-plane texture in terms of its intensity distribution as a function of the azimuthal angle ϕ. This is because that the preferred [110] direction happens to lie approximately in the plane of the film for the [111] textured CrN. Of all the grains that involve in the Bragg diffraction in a GIXS ϕ scan, some of them have the preferred in-plane orientation (i.e., their [110] direction points to the tangential direction with certain spread), whereas the others are randomly oriented azimuthally. For an azimuthal ϕ scan, the diffraction intensity at any ϕ is directly proportional to the volume fraction of the grains with the given in-plane orientation. Let V_f and V_r represent, respectively, the volume fractions of the grains with the preferred in-plane orientation and those with the random in-plane orientations. The V_f can be estimated by

$$V_f = \frac{V_f}{V_f + V_r} 100\% = \frac{\sum_{i=1}^{2} \int_{b_i}^{a_i} I(\phi) d\phi}{\int_0^{2\pi} I(\phi) d\phi} 100\%.$$

The denominator is the integrated diffraction intensity from the entire diffraction volume for a (220) ϕ scan by the GIXS geometry. The numerator is the integrated intensity of two peaks (i.e., from the total diffraction volume of the grains with the preferred in-plane orientation) of a (220) ϕ scan. Note that the treatment is not meant to be a generic quantification of the triaxial texture. The volume fraction V_f obtained hereby represents only an azimuthal component of the triaxial texture (i.e., in the plane of the film). Also the validity of the equation used here is only limited to the [111] textured CrN films from which the obtained (220) ϕ scans exhibit predominantly two intensity peaks, as indicated in Fig. 7.

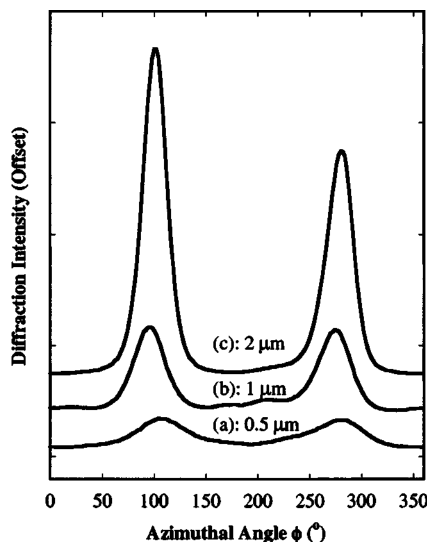

FIG. 5. The (220) scan results of the CrN films deposited at 460 W, 2 mTorr Ar partial pressure, and 1.2 mTorr nitrogen partial pressure, with varying film thickness.

Additionally, the half width at half maximum (HWHM) of an intensity peak is a measure of the angular spread of a given crystallographic orientation (namely, the degree of grain alignment) for the textured grains. Note the ϕ scan was performed at the grazing angle and the vertical divergence of the beam is only 0.2 mrad. Therefore, the HWHM represents primarily the azimuthal angular spread in the horizontal direction and the component in normal direction is negligible. In a sense, the volume fraction V_f and HWHM represents, respectively, the "quantity" and "quality" of the in-plane texture. Both of these were obtained by fitting the intensity peaks in Fig. 5 with Gaussian distributions. The results of the V_f and HWHM as functions of film thickness are shown in Fig. 6. Within the thickness range examined here, the in-plane texture appears to evolve in a complex matter, as re-

vealed by the distinct dependences on film thickness of V_f and HWHM between different stages of growth. One can roughly divide the texture evolution into two stages: from 0.5 μm to 1 μm and from 1 μm to 2 μm. In the first stage, both V_f and HWHM change rapidly, suggesting the concurrence of increased quantity and enhanced quality of the in-plane texture. In other words, the continuous outgrowth of randomly oriented grains by the in-plane textured grains and the grain alignment proceeded simultaneously in this stage. In the second stage, however, the V_f still increases continuously whereas the HWHM appears to reach a plateau quickly. Thus the evolution of the in-plane texture as the film grows thicker appears to proceed primarily by the continuous growth of in-plane textured grains while the degree of grain alignment appears to approach to a limit. This suggests that, in the second stage, the quantity and quality of the in-plane texture did not evolve with a same pace.

C. Effects of the nitrogen partial pressure

Previous studies have shown that adequate nitrogen flow is necessary to form textured CrN films.[17,18] Therefore only selected films that were deposited at relatively high nitrogen partial pressures were examined via azimuthal scans. Figure 7 shows the results for several CrN films deposited with three nitrogen partial pressures: 1.2 mTorr, 2.2 mTorr, and 2.8 mTorr. In view of the evolving nature of the in-plane texture, described in Sec. III B, all the CrN films had the same nominally thickness of 1 μm. The intensity distributions for the (220) and (113) reflections in Fig. 7 suggest that the CrN films deposited at varying nitrogen partial pressures exhibit the same type triaxial texture as denoted in Fig. 4. One may note the additional two small peaks that appeared for the films deposited at 2.2 mTorr and 2.8 mTorr nitrogen partial pressures, when compared with the film deposited at 1.2 mTorr nitrogen partial pressure. This difference, which has little significance, can be readily explained by considering small deviations of the preferred orientation [111] from the film normal. This is clearly indicated by the pole figures shown in Fig. 8. Such a deviation, if envisaged with the aid of Fig. 4, would be depicted as a tilt of [111] and [112] directions around the [110] axis. Since the ϕ scans were performed via symmetric GIXS geometry, the tilt with varying degrees caused either the presence or the absence of the additional peaks. As a matter of fact, if this were not the case, a (220) azimuthal scan would actually exhibit six peaks since there are six equivalent ⟨220⟩ crystallographic directions orthogonal to [111] in a cubic lattice. One can conclude that the CrN films deposited at varying nitrogen partial pressures developed the same type of triaxial texture. In Fig. 9, the volume fraction V_f and HWHM are shown as functions of nitrogen partial pressures. Note that once the nitrogen partial pressure reaches an adequate level for forming a single, stable CrN phase, both V_f and HWHM display little variations. This suggests that the evolution of the in-plane texture seems to be insensitive to the nitrogen partial pressure once the conditions to form the CrN phase are attained.

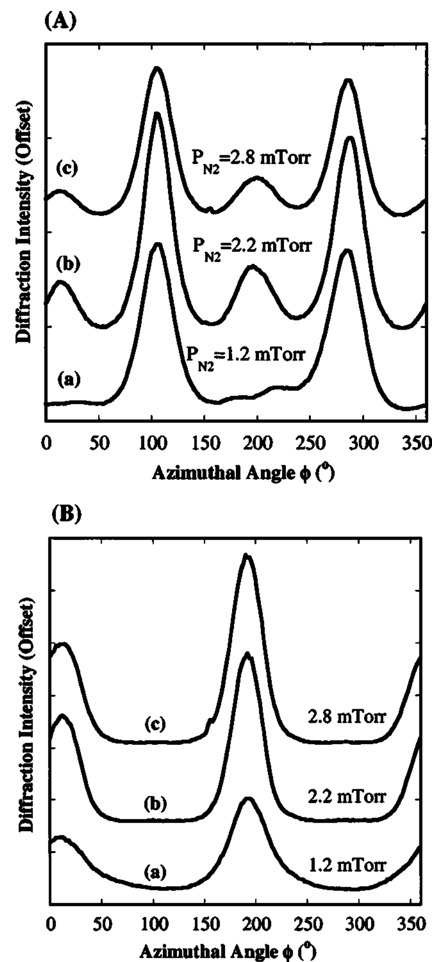

FIG. 7. Azimuthal scan results of the (220) reflection (a) and the (113) reflection (b) for the 1 μm thick films deposited at different nitrogen partial pressures. All other deposition parameters were kept the same: 460 W and 2 mTorr Ar partial pressure.

D. Growth morphologies and microstructures

Figure 10 shows the surface morphologies of selected chromium nitride films reactively sputtered at different levels of nitrogen partial pressures. Note that the films shown in Figs. 10(a) and 10(d) correspond to the conditions that lead to the formation of single, stable phases (either Cr or CrN). One can see that these films exhibit relatively high surface roughness with larger mounds. The films in Figs. 10(b) and 10(c), which were formed at the transitional region between the two stable phases, clearly exhibit reduced surface toughness. The TEM micrographs of Fig. 11 illustrate the evolution of microstructures. Notably, the films with a single, stable phase (again either Cr or CrN) developed well-organized microstructures with relatively coarse grain structures. Their selected area electron diffraction patterns indicate that the grains are largely aligned up crystallographically, leading to triaxially textured structures. This observation is consistent with the x-ray diffraction results described in Secs. III A–III C. Furthermore, the films deposited in the transitional region, shown in Figs. 11(b)–11(d), exhibit significantly refined macrostructures with diminished or no crystallographic textures. With a particular level of nitrogen partial pressure, nanostructured films

(a)

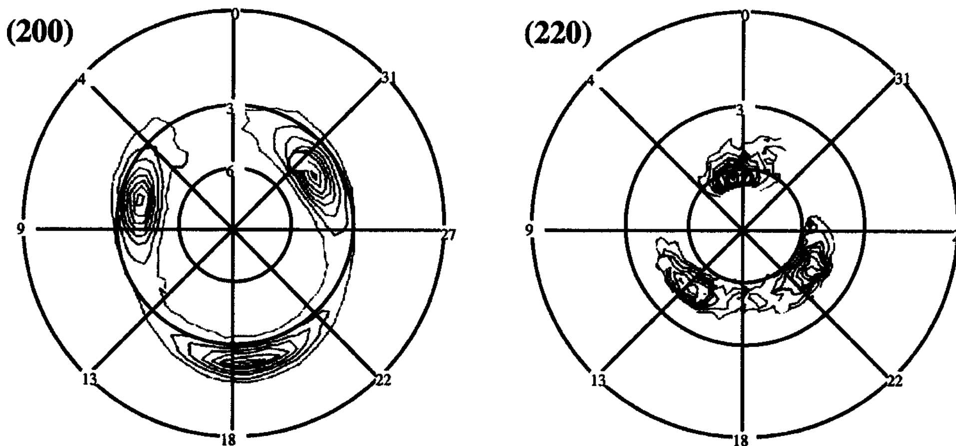

(b)

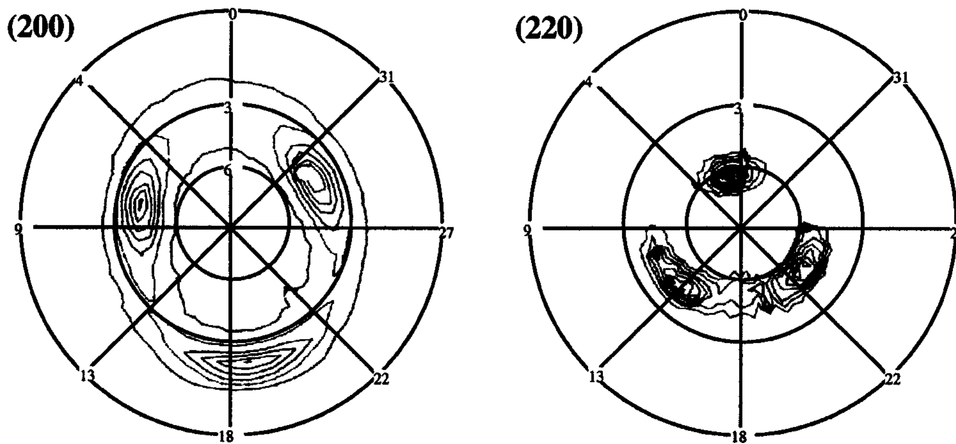

FIG. 8. The (200) and (220) pole figures of the 1 μm CrN films deposited at two different nitrogen partial pressures: 2.2 mTorr and 2.8 mTorr. All other deposition parameters were kept the same: 460 W and 2 mTorr Ar partial pressure.

[e.g., Fig. 11(c)], along with a sudden reversal of residual stress from tensile to compressive,[18] can be obtained.

Based on the observations in this work and those from previous studies,[12,17,18] the general characteristics of the reactively sputtered chromium nitride films can be summarized as shown in Figs. 10 and 11. The films are categorized in terms of microstructure, crystallographic texture, surface morphology, and residual stress. The distinct features of these films can be explained from two underlying growth regimes, which are the subject of the following section.

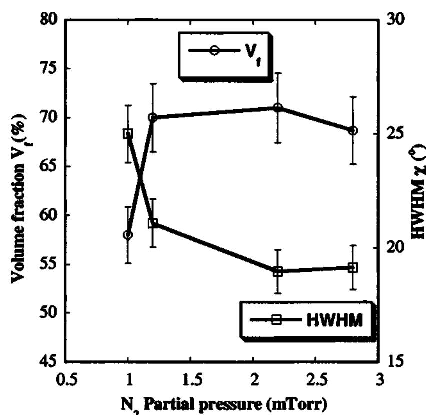

FIG. 9. Variations of the volume fraction V_f and the HWHM as functions of nitrogen partial pressure. Due to the grazing angle used in the ϕ scans, the data represent the results from the ~150 nm top layers of the films.

IV. DISCUSSION

Magnetron sputtered metal thin films deposited with a deposition geometry similar to that used in this work have been reported to develop in-plane textures in addition to out-of-plane textures.[11–14] The evolution of in-plane textures is explained by a model that incorporates both growth anisotropy and the self-shadowing effect.[15] In this work, it is shown that an in-plane texture can also develop in a multiple component thin film deposited via reactive sputtering. Other film characteristics such as microstructure, surface morphology, and residual stress appear to be closely linked to the crystallographic characteristics of the films. In the case of texture formation, this work, along with previous studies,[12,17,18] suggests that there are two growth regimes for

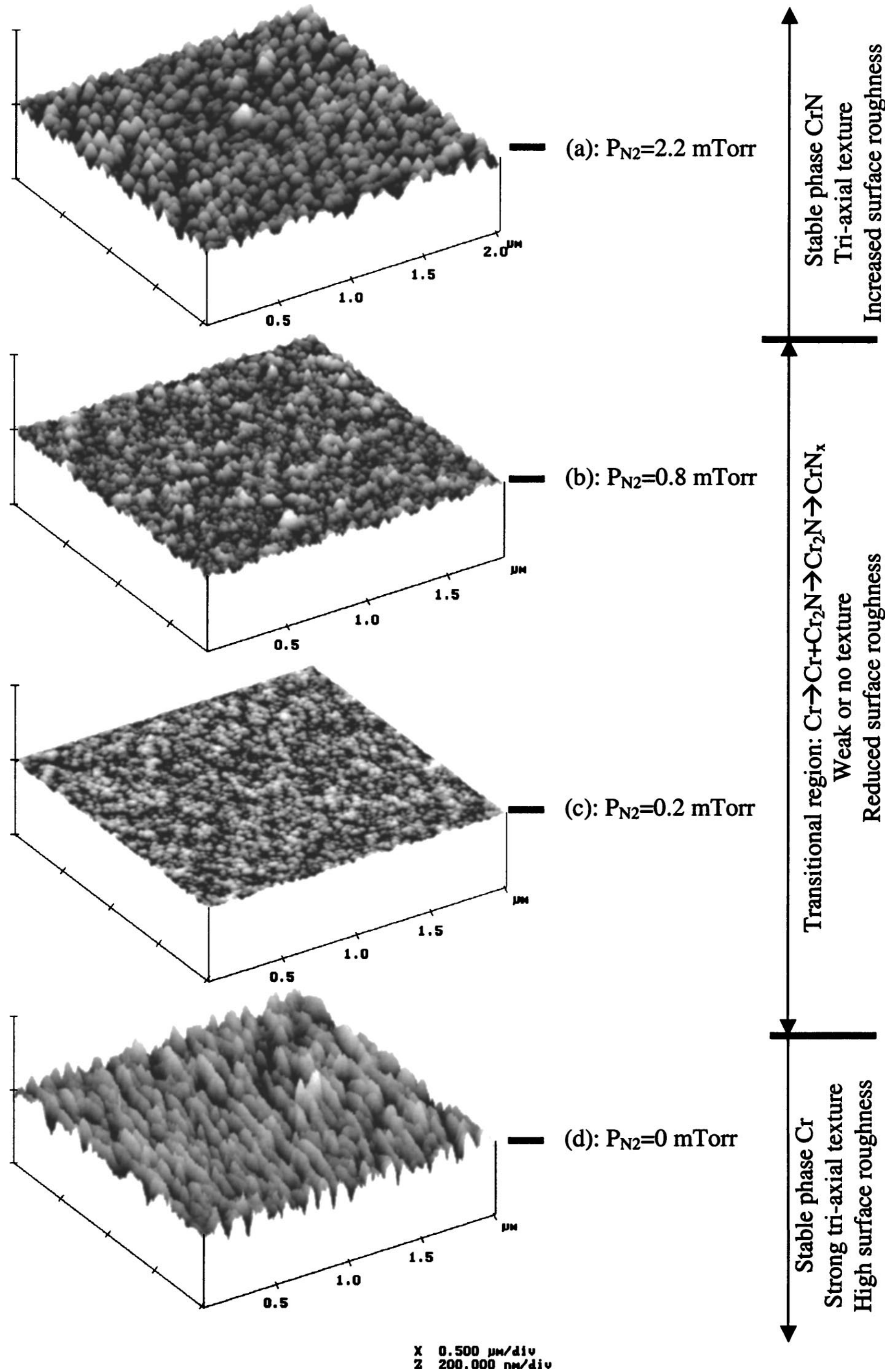

FIG. 10. AFM surface plots showing the growth morphologies of the films deposited at varying nitrogen partial pressures, which correspond to the different phase formation regimes.

the Cr–N system. The first one involves the deposition conditions that lead to in-plane textured films associated with formation of a single, stable phase. This includes both the films of pure Cr phase deposited in absence of nitrogen and the films of single, stöichiometric CrN phase deposited at given levels of nitrogen partial pressure. In this regime, the typical film characteristics include well-organized microstructures, relatively coarse grains that tend to align crystallographically, increased surface roughness and tensile residual stress. The second regime involves the transitional region between Cr and CrN, where levels of nitrogen are relatively low for attaining a single, stöichiometric phase of CrN. The films deposited in this regime show significantly weakened or no texture, as compared to the strongly textured films in the first regime. Phase analysis indicates that the films in the transition region consist of multiple phases of primarily Cr and Cr_2N or thermodynamically metastable, nonstöichiometric CrN_x.[17,18] The most notable characteristics of the films in the second regime are the significant microstructural refinements concurrently with decreasing growth roughness and lowering tensile stress. As a matter of fact, nanostructured chromium nitride films, with compressive stress,[18] were obtained with properly controlled levels of nitrogen partial pressure.

The distinct film characteristics between the two different growth regimes can be largely explained in light of the

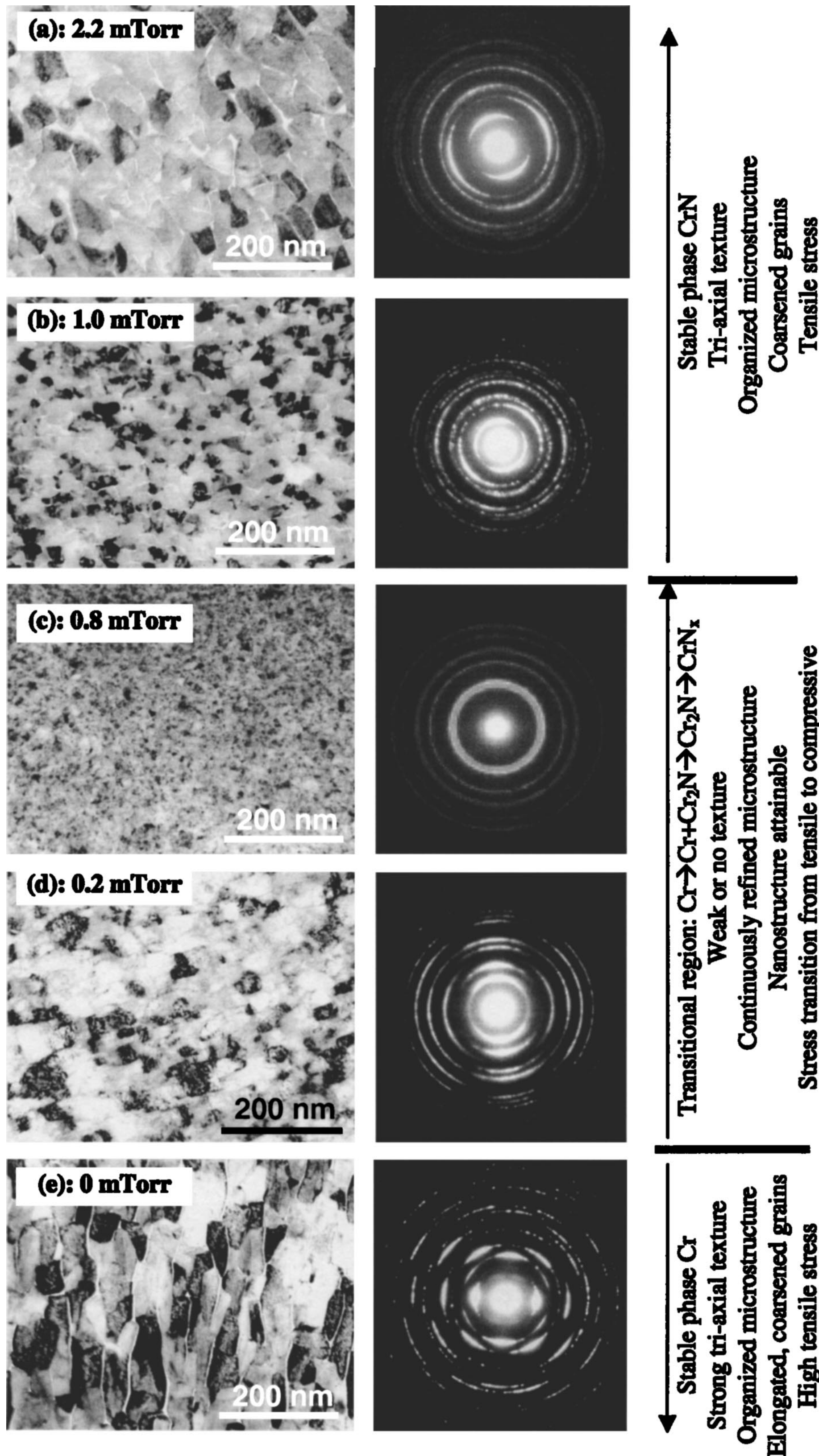

FIG. 11. TEM micrographs showing the evolution of the microstructures and the development of the in-plane texture, in relation to the different phase formation regimes.

structural zone models proposed for film growth.[16,19–21] Microstructural observations suggest that the textured films (both Cr and CrN) appear to exhibit Zone T type structures. In this regime, the film growth is dominated by significant surface diffusion of adatoms, which is sufficient to cause local epitaxy within individual growth columns. The film structure is characteristic of competitive grain growth and kinetic roughening. Through atomic shadowing, these effects become exacerbated due to the deposition geometry used in this work in which the flux of adatoms has varying angles (with respect to the plane of growth) as the substrate moves through underneath the cathode.[14] Accordingly the growth in this regime tends to lead to film characteristics manifested by organized microstructure, coarse grains with preferred crys-

tallographic orientations (i.e., texture) and rough surface morphology. All these are, in general, consistent with the observations of the single-phase films of either Cr or CrN.

The microstructures of the films in the second regime tend to transit to the type III microstructure.[16,20] The primary growth mechanism in this transitional region appears to be the disruption of local epitaxy, a key feature for the film growth in the first regime. This is closely related to the phase formation in this transitional region. Due to the presence of more than one phase (Cr, Cr_2N, and CrN_x), the microstructural evolution involves the repeated pileup of small, randomly oriented grains of different phase structures. Their continuous renucleations interrupt local epitaxial growth, which impedes competitive grain growth and kinetic roughening. As a result, the films exhibit characteristics such as significantly refined microstructure, weakened or no crystallographic texture, decreased surface roughness, and stress reversal from tensile to compressive.[18] In general, the observations made on the Cr–N system could likely be applied to other reactively sputtered systems. In fact, the impurity or reactive species as grain refiner for deposited films have been also reported in other systems.[16,20] The presence of the reactive species may be exploited as an additional tool for controlling microstructural evolution, texture development and other related characteristics of reactively sputtered films.

V. CONCLUSIONS

With the given deposition geometry, the reactively sputtered CrN films developed the in-plane texture, similar to sputtered metal thin films. The three preferred orientations were correlated to the characteristic directions associated with the deposition geometry. Two distinct growth regimes were identified for the Cr–N system through detailed examination of various film characteristics. The first one involves the conditions that form a single, stable phase (either Cr or CrN). In this regime, the film growth seems to be dominated by local epitaxy in individual columns, competitive grain growth, and kinetic roughening. This microscopic growth mechanism is manifested by the general film characteristics such as development of crystallographic texture, evolution of well-organized microstructure with relatively coarser grains, increased surface roughness, and large tensile stress. The second regime involves the transitional region between the stable phases Cr and CrN. In this regime, the film growth seems to proceed through continuous renucleations, which disrupt local epitaxy. As results, the films tend to exhibit weakened or no crystallographic texture, significant microstructural refinement, reduced surface roughness, and decreased tensile stress. In particular, nanostructured chromium nitride films with compressive stress (without bias voltage) could be obtained with properly controlled levels of nitrogen partial pressure.

ACKNOWLEDGMENTS

The U.S. Army Research Office, Research Triangle Park, NC, supported this research work under Grant No. DAAF19-02-1-0335. The support and encouragement from Dr. Larry Fehrenbacher of TAT, Inc. is gratefully acknowledged. The GIXS experiments were performed on Beamline 7-2 at SSRL, a DOE funded facility. The authors wish to thank Dr. Jeff Hershberger (Argonne National Lab), Dr. Jay Whitacre (JPL, Caltech), and Ms. Beth Ann Rainey (IBM) for their assistance in x-ray scattering experiments performed at SSRL. The author (Z.B.Z.) would also like to thank Dr. Mark Krage at Delphi Research Labs for reviewing the manuscript.

[1]D. P. Tracy, D. B. Knorr, and K. P. Rodbell, J. Appl. Phys. **76**, 2671 (1994).
[2]K. T. Lee, J. A. Szpunar, and D. B. Knorr, Mater. Sci. Forum **204–206**, 423 (1996).
[3]M. Kobayashi and Y. Doi, Thin Solid Films **128**, 259 (1984).
[4]A. N. Campbell, R. E. Mikawa, and D. B. Knorr, J. Electron. Mater. **22**, 589 (1993).
[5]M. R. Kim, S. Guruswamy, and K. E. Johnson, J. Appl. Phys. **74**, 4643 (1993).
[6]A. Kawamoto and F. Hikami, J. Appl. Phys. **69**, 5151 (1991).
[7]G. Knuyt, C. Quaeyhaegens, J. D'Haen, and L. M. Stals, Thin Solid Films **258**, 159 (1995).
[8]D. B. Knorr and J. A. Szpunar, JOM **46**, 42 (1994).
[9]J. M. E. Harper, K. P. Rodbell, E. G. Colgan, and R. H. Hammond, J. Appl. Phys. **82**, 4319 (1997).
[10]H. Ji, G. S. Was, J. W. Jones, and N. R. Moody, J. Appl. Phys. **81**, 6754 (1997).
[11]O. P. Karpenko, J. C. Bilello, and S. M. Yalisove, J. Appl. Phys. **76**, 4610 (1994).
[12]Z. B. Zhao, S. M. Yalisove, Z. U. Rek, and J. C. Bilello, J. Appl. Phys. **92**, 7183 (2002).
[13]M. A. Vill, Z. U. Rek, S. M. Yalisove, and J. C. Bilello, J. Appl. Phys. **78**, 3812 (1995).
[14]J. F. Whitacre, Z. U. Rek, J. C. Bilello, and S. M. Yalisove, J. Appl. Phys. **84**, 1346 (1998).
[15]O. P. Karpenko, J. C. Bilello, and S. M. Yalisove, J. Appl. Phys. **82**, 1397 (1997).
[16]I. Petrov, P. B. Bama, L. Hultman, and J. E. Greene, J. Vac. Sci. Technol. A **21**, S117 (2003).
[17]Z. B. Zhao, Z. U. Rek, S. M. Yalisove, and J. C. Bilello, Surf. Coat. Technol. **185**, 329 (2004).
[18]Z. B. Zhao, Z. U. Rek, S. M. Yalisove, and J. C. Bilello, Thin Solid Films **472**, 96 (2005).
[19]B. A. Movchan and A. V. Demchishin, Fiz. Met. Metalloved. **28**, 83 (1969).
[20]P. B. Barna and M. Adamik, Thin Solid Films **317**, 27 (1998).
[21]C. R. M. Grovenor, H. T. G. Hentzell, and D. A. Smith, Acta Metall. **32**, 773 (1984).